



Article

Prescribed-Time Projective Synchronization for Different Dimensional Complex Networks via Fuzzy Reinforcement Learning

Xin Qu and Tao Dong *

Chongqing Key Laboratory of Nonlinear Circuits and Intelligent Information Processing, College of Electronics and Information Engineering, Southwest University, Chongqing 400715, China

* Correspondence: david312@swu.edu.cn

How To Cite: Qu, X.; Dong, T. Prescribed-Time Projective Synchronization for Different Dimensional Complex Networks via Fuzzy Reinforcement Learning. *Journal of Machine Learning and Information Security* 2026, 2(1), 2. <https://doi.org/10.53941/jmlis.2026.100002>

Received: 14 September 2025

Revised: 21 November 2025

Accepted: 12 January 2026

Published: 26 January 2026

Abstract: This paper investigates the prescribed-time projective synchronization (PTPS) for complex networks (CNs) with different dimension. To solve this problem, a projective synchronization error is constructed and a novel performance value function integrated with the prescribed time and desired accuracy is proposed. Subsequently, a fuzzy controller is introduced to address the prescribed-time projective synchronization issue. The controller is realized through a fuzzy adaptive dynamic programming (ADP)-based framework. Additionally, the convergence analysis of the proposed methodology is provided, demonstrating that the projective synchronization error can converge to a predefined residual set within the prescribed time, which means the synchronization of CNs is solved. Finally, a numerical example is presented to verify the obtained results.

Keywords: prescribed-time; complex networks; projective synchronization; fuzzy fuzzy reinforcement learning

1. Introduction

Recently, complex networks (CNs) have received a lot of attentions due to their widely applications in many fields such as power grids, social networks, transportation systems and so on [1–5]. Synchronization has been the research focus of CNs. It refers to the phenomenon where nodes in two CNs gradually adjust from different initial states and eventually reach a consistent state through control. To achieve synchronization, a variety of control strategies have been proposed such as event-triggered control strategy [6–9], finite-time control strategy [10–12], adaptive control strategy [13–16], and impulsive control strategy [17–20].

Reinforcement learning (RL) is a powerful machine learning technique that systematically adjusts an agent's behavior based on observed environmental responses. Due to the fact that reinforcement learning algorithms do not require knowledge of the system's dynamic model, they are widely used in complex network synchronization [21–32]. In [21], a secure RL algorithm is proposed to address the secure synchronization problem of two-time-scale CNs under malicious attacks. In [22], a distributed RL algorithm is proposed to address the synchronization problem of CNs. In [23,24], a two-level value iteration algorithm is proposed to solve the synchronization problem of CNs. In [26], a data-based off-policy RL algorithm is proposed to solve the synchronization of CNs with input saturation. In [25,28,29], three cluster synchronization methods based on state-flipped control and QL algorithm is proposed to solve the cluster synchronization of the Boolean network. In [30], an RL-based control method is proposed to address the synchronization of CNs with unknown non-identical dynamics. In [32], a synchronization control method based on RL and Graph Convolution Networks is proposed to address the synchronization of complex networks [33–35,38–41]. It can be seen that, although many RL-based algorithms have been proposed to solve synchronization problems for various CNs, there is still little research on prescribed-time synchronization of CNs. Prescribed-time synchronization is that CNs can achieve synchronization within a predefined time by designing control algorithms.

Inspired by the above discussion, this paper studies the PTPS of two different dimension CNs via fuzzy RL.



The main contributions of this paper are as follows:

1. A projective synchronization error is constructed and a novel performance value function integrated with the predefined time horizon and desired accuracy is proposed. This pivotal step translates the challenge of achieving projective synchronization within a predefined time into an optimal regulation problem.
2. A novel controller is proposed to solve the prescribed-time projective synchronization problem. A fuzzy ADP-based framework is used to realize the controller. Moreover, the convergence analysis of the proposed algorithm is given, which shows that the projective synchronization error can converge to the predesigned residual set within a prescribed time.

The remainder of this paper is organized as follows: Section 2 presents the system model and problem formulation. Section 3 develops the prescribed-time control strategy. Section 4 provides the main results. Section 5 offers numerical simulations to validate the proposed approach.

2. Problem Description and Some Preliminaries

2.1. Model Description

Consider two CNs: driving network and response network. The driving network consists of N nodes. The dynamic of each node is described as follows:

$$\dot{\zeta}_i = f_i(\zeta_i) + \sum_{j=1}^N a_{ij} H_1 \zeta_j \quad (i = 1, 2, \dots, N), \tag{1}$$

where $\zeta_i \in R^n$ is the i th node state, $f_i(\cdot) \in R^n$ is the i th node dynamic, $H_1 \in R^{n \times n}$ is the inner coupling matrix, a_{ij} is the connection weight from node i to node j ($i \neq j$).

The response network tracking the driving system also consists of N nodes. The state of each node is an m -dimensional vector, and the dynamic of i node is described as follows:

$$\dot{\xi}_i = z_i(\xi_i) + \sum_{j=1}^N c_{ij} H_2 \xi_j + g_i(\xi_i) u_i, \tag{2}$$

where $\xi_i \in R^m$ is the i th state of the node, which is an m -dimension vector, $z_i(\cdot) \in R^m$ is the i th system dynamic, which is unknown, $H_2 \in R^{m \times m}$ is the internal coupling matrix, $g_i(\cdot) \in R^{m \times m}$ is the control gain, u_i is the control input, and c_{ij} is the connection weight from node i to node j ($i \neq j$).

Assumption 1. (1) $g_i(\cdot)$ are bounded, i.e. $\|g_i(\cdot)\| \leq g_{M,i}$, where $g_{M,i} > 0$. (2) $f_i(\cdot)$, $z_i(\cdot)$, $g_i(\cdot)$ are Lipschitz continuous.

Define a projective synchronization error as:

$$e_i = \xi_i - \mathcal{B}\zeta_i, \tag{3}$$

where $\mathcal{B} \in R^{m \times n}$ and $e_i \in R^m$ is a projective matrix.

By (1) and (2), one has

$$\begin{aligned} \dot{e}_i &= \dot{\xi}_i - \mathcal{B}\dot{\zeta}_i \\ &= \mathcal{F}_i(e_i) + g_i(\xi_i)u_i, \end{aligned} \tag{4}$$

where $\mathcal{F}_i(e_i) = z_i(\xi_i) - \mathcal{B}f_i(\zeta_i) + \sum_{j=1}^N (c_{ij}H_2\xi_j - a_{ij}\mathcal{B}H_1\zeta_j)$.

Definition 1. For a pre-defined time T and a pre-defined accuracy $0 < \tau < 1$, if $\lim_{t \rightarrow T} \|e_i\| < \tau$ holds, the PTPS of (1) and (2) can be achieved.

Define a piecewise function as:

$$p = \begin{cases} (1 - \tau) \left(\frac{T-t}{T}\right)^2 + \tau, & 0 \leq t < T \\ \tau, & t \geq T, \end{cases} \tag{5}$$

where $T > 0$ is the pre-defined time and $\tau > 0$ is the pre-defined accuracy.

Lemma 1. p defined in (5) has two properties: (1) $p(0) = 1$ and p is strictly decreasing on $[0, T]$; (2) p is smooth, p and \dot{p} are bounded for all $t \geq 0$.

Proof: See Appendix A.

Define a transformation function:

$$y_i = \tan\left(\frac{\pi e_i}{2p}\right), \tag{6}$$

where $y_i = [y_{i1}, \dots, y_{im}]^T \in R^m$, $|e_{i\ell}(0)| < p(0)$, $\ell = 1, \dots, m$. m denotes the dimension of e_i .

By (6), if $y_{i\ell}$ is bounded and $-p(0) < e_{i\ell}(0) < p(0)$, then one has $-p < e_{i\ell} < p$. According to Lemma 1, one has $-p < e_{i\ell} < p$ for $\forall t \geq T$, which means that if $-p(0) < e_{i\ell}(0) < p(0)$ is satisfied and the bounded of p is guaranteed, $\lim_{t \rightarrow T} \|e_i\| < \tau$ holds.

By (4) and (6), one has

$$\begin{aligned} \dot{y}_i &= \frac{\pi}{2p} \left[(1 + y_{i1}^2) \left(\dot{e}_{i1} - \frac{\dot{p}}{p} e_{i1} \right), \dots, (1 + y_{im}^2) \left(\dot{e}_{im} - \frac{\dot{p}}{p} e_{im} \right) \right]^T \\ &= \bar{\lambda}_i \left(\mathcal{F}_i(e_i) + g_i(\xi_i) u_i - \frac{\dot{p}}{p} e_i \right), \end{aligned} \tag{7}$$

where $\bar{\lambda}_i = \text{diag} \left\{ \frac{\pi}{2p} (1 + y_{i1}^2), \dots, \frac{\pi}{2p} (1 + y_{im}^2) \right\}$.

2.2. Fuzzy Logic System

For a FLS, the fuzzy rule R_k is defined as:

IF: z_1 is F_1^k, \dots, z_l is $F_l^k, k = 1, \dots, K$

THEN: y_B is B^k

where, K is the number of fuzzy rules and $z = [z_1, \dots, z_l]^T$ is the input of the FNN. F_i^k and B^k are the fuzzy sets. y_B is the output of FNN, which is defined as $y_B(z) = \frac{\sum_{l=1}^K \Psi^k \prod_{i=1}^l \mu_{F_i^k}(z_i)}{\sum_{k=1}^K \left[\prod_{i=1}^l \mu_{F_i^k}(z_i) \right]}$, where $\mu_{F_i^k}(z_i)$ is the membership function of F_i^k , Ψ^k satisfies $\mu_{B^k}(\Psi^k) = \max_{y_B \in R} \mu_{B^k}(y_B)$. Let $\Psi = [\Psi^1, \dots, \Psi^K]^T$, $\Phi = [\Phi^1, \dots, \Phi^K]^T$, and $\Phi^k = \frac{\prod_{i=1}^l \mu_{F_i^k}(z_i)}{\sum_{k=1}^K \left[\prod_{i=1}^l \mu_{F_i^k}(z_i) \right]}$, one has $y_B(z) = \Psi^T(z)\Phi$.

Lemma 2. (See [36]): For any $\rho > 0$, there exists fuzzy logic system (FLS) $\Psi^T(z)\Phi$ and defined a continuous function $h(z)$ on a compact set Ξ , can $\sup_{z \in \Xi} |h(z) - \Psi^T(z)\Phi| \leq \rho$.

3. Prescribed-Time Synchronization Control Design

Define a performance value function as:

$$J_i(y_i) = \int_t^\infty r(y_i(\tau), u_i(\tau)) d\tau, \tag{8}$$

where $r_i(y_i, u_i) = y_i^T Q_i y_i + u_i^T R_i u_i$, Q_i and R_i are positive definite matrices. The optimal value of (8) is:

$$J_i^*(y_i) = \min_{u \in \Psi(\Omega)} \int_t^\infty r(y_i(\tau), u_i(\tau)) d\tau. \tag{9}$$

By (9), one can obtain:

$$\begin{aligned} H_i(y_i, u_i, \nabla J_i) &= \\ \nabla J_i^T \cdot \left(\bar{\lambda}_i \left(\mathcal{F}_i(e_i) + g_i(\xi_i) u_i - \frac{\dot{p}}{p} e_i \right) \right) &+ r(y_i, u_i). \end{aligned} \tag{10}$$

Then, we have

$$\min_{u \in \Psi(\Omega)} \{H_i(y_i, u_i, \nabla J_i^*)\} = 0, \tag{11}$$

where $\nabla J_i^* = \partial J_i^* / \partial y_i$. The optimal control policies is as follows:

$$u_i^* = -\frac{1}{2}R_i^{-1}g_i^T(\xi_i)v_i, \tag{12}$$

where $v_i = \bar{\lambda}_i \nabla J_i^*$. Substituting (12) into (11), one has:

$$y_i^T Q_i y_i + v_i^T \left(\mathcal{F}_i - \frac{\dot{p}}{p} e_i \right) - \frac{1}{4} v_i^T g_i R_i^{-1} g_i^T v_i = 0, \tag{13}$$

with $J_i^*(0) = 0$.

In the following we use fuzzy actor-critic framework to realize the controller. The control diagram is given in Figure 1.

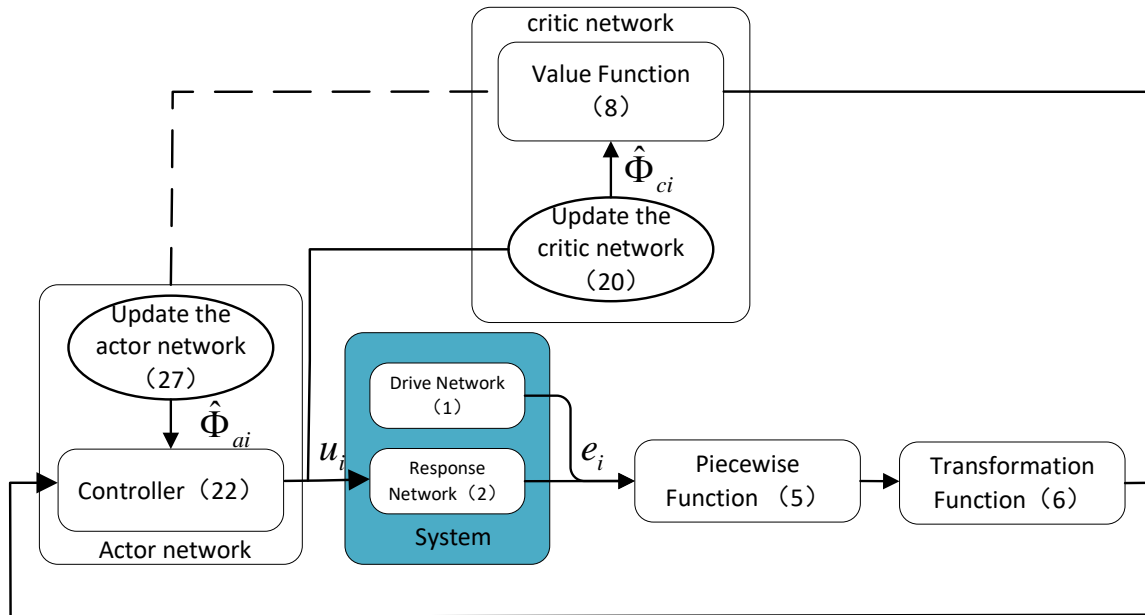


Figure 1. The control system.

3.1. Critic Network Design

By Lemma 2, we know that the FLS can approximate any function. Therefore, we use FLS to build critic network. The critic network is used to approximate v_i , which is described as

$$v_i(Z_i) = \Psi_i^T(Z_i)\Phi_i + \varepsilon_i(Z_i), \tag{14}$$

where $Z_i = [e_i, p_i, y_i]^T$, $\Phi_i \in R^l$, l where l is the number of fuzzy rules and $\Psi_i \in R^{l \times n}$ is the basis function matrix. The optimal parameter vector and the approximation error are denoted as Φ_i and $\varepsilon_i \in R^n$, respectively. The error ε_i satisfies $\|\varepsilon_i\| \leq \delta$; where δ is a constant, $\|\Psi_i\| \leq c_\Psi$ with $c_\Psi > 0$.

By (14), one has

$$\begin{aligned} \varepsilon_{H_i} = H_i(y_i, u_i, \Phi_i) &= y_i^T Q_i y_i + u_i^T R_i u_i + \Phi_i^T \Psi_i(Z_i) \\ &\times \left(\mathcal{F}_i(e_i) + g_i(\xi_i) u_i - \frac{\dot{p}}{p} e_i \right), \end{aligned} \tag{15}$$

where $\varepsilon_{H_i} = -\varepsilon_i^T \left(\mathcal{F}_i(e_i) + g_i(\xi_i) u_i - \frac{\dot{p}}{p} e_i \right)$. Then, one can obtain:

$$\hat{v}_i(Z_i) = \Psi_i^T(Z_i)\hat{\Phi}_{ci}, \tag{16}$$

where $\hat{v}_i(Z_i)$, $\hat{\Phi}_{ci}$ are the estimate $v_i(Z_i)$. Therefore, we can further obtain that

$$\begin{aligned} \varepsilon_{B_i} = H_i(y_i, u_i, \hat{\Phi}_{ci}) &= y_i^T Q_i y_i + u_i^T R_i u_i + \hat{\Phi}_{ci}^T \Psi_i(Z_i) \\ &\times \left(\mathcal{F}_i(e_i) + g_i(\xi_i) u_i - \frac{\dot{p}}{p} e_i \right). \end{aligned} \tag{17}$$

The weight estimation error is defined as:

$$\tilde{\Phi}_{ci} = \Phi_i - \hat{\Phi}_{ci}. \tag{18}$$

Then, one has

$$\varepsilon_{B_i} = (\tilde{\Phi}_{ci} - \varepsilon_i^T) \left(\mathcal{F}_i(e_i) + g_i(\xi_i) u_i - \frac{\dot{p}}{p} e_i \right).$$

Define the error function:

$$E_{B_i} = \frac{1}{2} \varepsilon_{B_i}^2. \tag{19}$$

From (19), the update law of the critic system is designed as:

$$\begin{aligned} \dot{\hat{\Phi}}_{ci} &= -\frac{\varpi_{1i}}{(\lambda_i^T \lambda_i + 1)^2} \frac{\partial E_{B_i}}{\partial \hat{\Phi}_{ci}} \\ &= -\frac{\varpi_{1i} \lambda_i}{(\lambda_i^T \lambda_i + 1)^2} \left[\lambda_i^T \hat{\Phi}_{ci} + y_i^T Q_i y_i + u_i^T R_i u_i \right], \end{aligned} \tag{20}$$

where $\lambda_i = \Psi_i \left(\mathcal{F}_i(e_i) + g_i(\xi_i) u_i - \frac{\dot{p}}{p} e_i \right)$, $\varpi_{1i} > 0$ is the learning rate.

3.2. Action Network Design

By (12), the idea control input u_i^* is:

$$u_i^* = -\frac{1}{2} R_i^{-1} g_i^T(\xi_i) \Psi_i^T(Z_i) \Phi_i. \tag{21}$$

where Φ_i is unknown. The actor network is also a FLS, which is used to approximate u_i^* :

$$\hat{u}_i = -\frac{1}{2} R_i^{-1} g_i^T(\xi_i) \Psi_i^T(Z_i) \hat{\Phi}_{ai}, \tag{22}$$

where $\hat{\Phi}_{ai}$ is the current estimated value of Φ_i in (21). Then, we have:

$$\begin{aligned} \varepsilon_{HJB_i} &= y_i^T Q_i y_i + \Phi_i^T \Psi_i(Z_i) \left(\mathcal{F}_i - \frac{\dot{p}}{p} e \right) \\ &\quad - \frac{1}{4} \Phi_i^T \Psi_i(Z_i) g_i R_i^{-1} g_i^T \Psi_i^T(Z_i) \Phi_i. \end{aligned} \tag{23}$$

where

$$\varepsilon_{HJB_i} = \varepsilon_i^T \left(\mathcal{F}_i - \frac{\dot{p}}{p} e \right) + \frac{1}{2} \Phi_i^T \Psi_i g_i R_i^{-1} g_i^T \varepsilon_i + \frac{1}{4} \varepsilon_i^T g_i R_i^{-1} g_i^T \varepsilon_i.$$

The estimation error is:

$$\tilde{\Phi}_{ai} = \Phi_i - \hat{\Phi}_{ai}. \tag{24}$$

Let $\tilde{u}_i = u_i^* - \hat{u}_i$. By (24), the error of the action network can be rewritten as:

$$\begin{aligned} \varepsilon_{A_i} &= \varepsilon_i^T \left(\mathcal{F}_i - \frac{\dot{p}}{p} e \right) + \frac{1}{2} (\Phi_i - \hat{\Phi}_{ai})^T \Psi_i g_i R_i^{-1} g_i^T \varepsilon_i \\ &\quad + \frac{1}{4} \varepsilon_i^T g_i R_i^{-1} g_i^T \varepsilon_i. \end{aligned} \tag{25}$$

Define the mean square error is:

$$E_{A_i} = \frac{1}{2} \varepsilon_{A_i}^2. \tag{26}$$

The update law of the action network is designed as:

$$\dot{\hat{\Phi}}_{ai} = -\varpi_{2i} \left[\left(\iota_{ai} \hat{\Phi}_{ai} - \iota_{ci} \bar{\vartheta}_i^T \hat{\Phi}_{ci} \right) - \frac{1}{4} \theta_i(Z_i) \hat{\Phi}_{ai} \vartheta_i^T(Z_i) \hat{\Phi}_{ci} \right], \tag{27}$$

where $\varpi_{2i} > 0$ is the learning rate, $\theta_i(Z_i) = \Psi_i g_i R_i^{-1} g_i^T \Psi_i^T$, $\vartheta_i(Z_i) = \frac{\lambda_i}{(\lambda_i^T \lambda_i + 1)^2}$, $\iota_{ai} > 0$ and $\iota_{ci} > 0$ are tuning parameters, $\bar{\vartheta}_i = \frac{\lambda_i}{(\lambda_i^T \lambda_i + 1)}$.

Thus, we propose a novel algorithm for the task, namely the Prescribed-Time Synchronization Control Design. The detailed procedure is summarized in Algorithm 1.

Algorithm 1 Prescribed-Time Synchronization Control Design

Input: prescribed time T , convergence accuracy $0 < \tau < 1$, matrices $Q_i > 0, R_i > 0$
Initialization: state $\zeta_i(0)$ and $\xi_i(0)$, critic weight $\Phi_c(0)$, and actor weight $\Phi_a(0)$
Parameters: learning rates $\varpi_1 > 0$ and $\varpi_2 > 0$; tuning parameters $\iota_{ai} > 0$ and $\iota_{ci} > 0$
for $i = 1, \dots, n$
 By (3), compute e_i
 By (5), compute p
 By (6), compute y_i
 Define fuzzy IF-THEN rules, input $Z_i = [e_i, p, y_i]^T$, determine fuzzy basis function $\Psi(Z_i)$
 By (22), compute u_i
 Update Φ_{ci}
 Update Φ_{ai}
end for

4. Main Theoretical Results

In this section, the main theoretical results are given.

Theorem 1. For CNs (1) and (2) with the action network (21) and critic network (16), along with weight law of the critic network in (20) and the action network in (27), it is guaranteed that the $\lim_{t \rightarrow T} \|e_i\| < \tau$, which means the projective synchronization of (1) and (2) can be achieved.

Proof. Consider the following Lyapunov function:

$$V_i = J(y_i) + \frac{1}{2}Tr \left\{ \tilde{\Phi}_{ci}^T \kappa_{1i}^{-1} \tilde{\Phi}_{ci} \right\} + \frac{1}{2}Tr \left\{ \tilde{\Phi}_{ai}^T \kappa_{1i}^{-1} \tilde{\Phi}_{ai} \right\}. \tag{28}$$

Then

$$\begin{aligned} \dot{V}_i &= (\nabla J_i^T \bar{\lambda}_i^{-1}) \bar{\lambda}_i \left(\mathcal{F}_i(e_i) + g_i(\xi_i) u_i - \frac{\dot{p}}{p} e_i \right) \\ &+ \tilde{\Phi}_{ci}^T \frac{\lambda_i}{(\lambda_i^T \lambda_i + 1)^2} \left(\lambda_i^T \hat{\Phi}_{ci} + y_i^T Q_i y_i + \frac{1}{4} \hat{\Phi}_{ai}^T \theta_i(Z_i) \hat{\Phi}_{ai} \right) \\ &+ \hat{\Phi}_{ai} \left((\iota_{ai} \hat{\Phi}_{ai} - \iota_{ci} \bar{v}_i^T \hat{\Phi}_{ci}) - \frac{1}{4} \theta_i(Z_i) \hat{\Phi}_{ai} \vartheta_i^T(Z_i) \hat{\Phi}_{ci} \right). \end{aligned} \tag{29}$$

Let $\lambda_{1i} \equiv \Psi_i(Z_i) \left(\mathcal{F}_i(e_i) + g_i(\xi_i) u_i - \frac{\dot{p}}{p} e_i \right)$, one has

$$\Phi_i^T \lambda_{1i} = -y_i^T Q_i y_i - \frac{1}{4} \hat{\Phi}_i^T \theta_i(Z_i) \hat{\Phi}_{ai} + \varepsilon_{HJB_i}. \tag{30}$$

By (30), one has

$$\begin{aligned} \dot{V}_i &= (\bar{\lambda}_i \nabla J_i)^T \left(\mathcal{F}_i(e_i) + g_i(\xi_i) u_i - \frac{\dot{p}}{p} e_i \right) \\ &+ \tilde{\Phi}_{ci}^T \frac{\lambda_i}{(\lambda_i^T \lambda_i + 1)^2} \left(\lambda_i^T \hat{\Phi}_{ci} + y_i^T Q_i y_i + \frac{1}{4} \hat{\Phi}_{ai}^T \theta_i(Z_i) \hat{\Phi}_{ai} \right. \\ &\left. - \Phi_i^T \lambda_{1i} - y_i^T Q_i y_i - \frac{1}{4} \hat{\Phi}_i^T \theta_i(Z_i) \hat{\Phi}_{ai} + \varepsilon_{HJB_i} \right) \\ &+ \tilde{\Phi}_{ai} \left((\iota_{ai} \hat{\Phi}_{ai} - \iota_{ci} \bar{v}_i^T \hat{\Phi}_{ci}) - \frac{1}{4} \theta_i(Z_i) \hat{\Phi}_{ai} \vartheta_i^T(Z_i) \hat{\Phi}_{ci} \right). \end{aligned} \tag{31}$$

By using (17), from $\lambda_i = \Psi_i \left(\mathcal{F}_i(e_i) + g_i(\xi_i) \hat{u}_i - \frac{\dot{p}}{p} e_i \right)$ and $\lambda_{1i} \equiv \Psi_i(Z_i) \left(\mathcal{F}_i(e_i) + g_i(\xi_i) u_i - \frac{\dot{p}}{p} e_i \right)$, we have

$$\begin{aligned} \lambda_i^T \hat{\Phi}_{ci} - \Phi_i^T \lambda_{1i} &= -\tilde{\Phi}_{ci}^T \Psi_i(Z_i) \left(\mathcal{F}_i(e_i) - \frac{\dot{p}}{p} e_i \right) \\ &- \frac{1}{2} \hat{\Phi}_{ai} \theta_i^T(Z_i) \hat{\Phi}_{ci} + \frac{1}{2} \Phi_i \theta_i^T(Z_i) \hat{\Phi}_{ci}. \end{aligned} \tag{32}$$

Then, by combining (14) and (32), (31) can be expressed as

$$\begin{aligned} \dot{V}_i &= \Phi_i^T \Psi_i(Z_i) \left(\mathcal{F}_i(e_i) + g_i(\xi_i) u_i - \frac{\dot{p}}{p} e_i \right) + \tilde{\Phi}_{ci}^T \frac{\lambda_i}{(\lambda_i^T \lambda_i + 1)^2} \\ &\times \left(\lambda_i^T \hat{\Phi}_{ci} + y_i^T Q_i y_i + \frac{1}{4} \hat{\Phi}_{ai}^T \theta_i(Z_i) \hat{\Phi}_{ai} + \varepsilon_{HJB_i} - \tilde{\Phi}_{ci}^T \Psi_i(Z_i) \right. \\ &\times \left. \left(\mathcal{F}_i(e_i) - \frac{\dot{p}}{p} e_i \right) - \frac{1}{2} \hat{\Phi}_{ai} \theta_i^T(Z_i) \hat{\Phi}_{ci} + \frac{1}{2} \Phi_i \theta_i^T(Z_i) \Phi_i \right) \\ &+ \tilde{\Phi}_{ai}^T \left(\left(\iota_{ai} \hat{\Phi}_{ai} - \iota_{ci} \bar{\vartheta}_i^T \hat{\Phi}_{ci} \right) - \frac{1}{4} \theta_i(Z_i) \hat{\Phi}_{ai} \vartheta_i^T(Z_i) \hat{\Phi}_{ci} \right) \\ &+ \varepsilon_i^T(Z_i) \left(\mathcal{F}_i(e_i) + g_i(\xi_i) u_i - \frac{\dot{p}}{p} e_i \right). \end{aligned} \tag{33}$$

From $\tilde{\Phi}_{ci} = \Phi_i - \hat{\Phi}_{ci}$ and $\tilde{\Phi}_{ai} = \Phi_i - \hat{\Phi}_{ai}$, we have

$$\begin{aligned} &\tilde{\Phi}_{ai}^T \left(\iota_{ai} \hat{\Phi}_{ai} - \iota_{ci} \bar{\vartheta}_i^T \hat{\Phi}_{ci} \right) \\ &= \tilde{\Phi}_{ai}^T \iota_{ai} \Phi_i - \tilde{\Phi}_{ai}^T \iota_{ai} \tilde{\Phi}_{ai} - \tilde{\Phi}_{ai}^T \iota_{ci} \bar{\vartheta}_i^T \Phi_i + \tilde{\Phi}_{ai}^T \iota_{ci} \bar{\vartheta}_i^T \tilde{\Phi}_{ci}. \end{aligned} \tag{34}$$

So,

$$\begin{aligned} &\frac{1}{4} \hat{\Phi}_{ai}^T \theta_i(Z_i) \hat{\Phi}_{ai} - \frac{1}{4} \Phi_i^T \theta_i(Z_i) \Phi_i \\ &= \frac{1}{4} \tilde{\Phi}_{ai}^T \theta_i(Z_i) \tilde{\Phi}_{ai} - \frac{1}{2} \tilde{\Phi}_{ai}^T \theta_i(Z_i) \Phi_i. \end{aligned} \tag{35}$$

And,

$$\begin{aligned} &-\frac{1}{2} \hat{\Phi}_{ai}^T \theta_i(Z_i) \hat{\Phi}_{ci} + \frac{1}{2} \Phi_i^T \theta_i(Z_i) \Phi_i \\ &= \frac{1}{2} \Phi_i^T \theta_i(Z_i) \tilde{\Phi}_{ci} + \frac{1}{2} \tilde{\Phi}_{ai}^T \theta_i(Z_i) \Phi_i - \frac{1}{2} \tilde{\Phi}_{ai}^T \theta_i(Z_i) \tilde{\Phi}_{ci} \\ &= \frac{1}{2} \tilde{\Phi}_{ai}^T \theta_i(Z_i) \Phi_i + \frac{1}{2} \hat{\Phi}_{ai}^T \theta_i(Z_i) \tilde{\Phi}_{ci}. \end{aligned} \tag{36}$$

Substituting (30), (31), and (32) into (29) and combining (18), one has

$$\begin{aligned} \dot{V}_i &= \Phi_i^T \Psi_i(Z_i) \left(\mathcal{F}_i(e_i) + g_i(\xi_i) u_i - \frac{\dot{p}}{p} e_i \right) + \varepsilon_i^T(Z_i) \\ &\times \left(\mathcal{F}_i(e_i) - \frac{1}{2} g_i(\xi_i) R_i^{-1} g_i^T(\xi_i) \Psi_i^T(Z_i) \hat{\Phi}_{ai} - \frac{\dot{p}}{p} e_i \right) \\ &- \frac{\Phi_i^T \Psi_i(Z_i)}{2} g_i(\xi_i) R_i^{-1} g_i^T(\xi_i) \Psi_i^T(Z_i) \hat{\Phi}_{ai} \\ &+ \tilde{\Phi}_{ci}^T \frac{\lambda_i}{(\lambda_i^T \lambda_i + 1)^2} \left(\frac{1}{4} \hat{\Phi}_{ai}^T \theta_i(Z_i) \hat{\Phi}_{ai} + \varepsilon_{HJB_i} \right. \\ &+ \frac{1}{2} \hat{\Phi}_{ai}^T \theta_i(Z_i) \tilde{\Phi}_{ci} - \left. \left(\mathcal{F}_i(e_i) - \frac{\dot{p}}{p} e_i \right)^T \Psi_i^T(Z_i) \tilde{\Phi}_{ci} \right) \\ &- \frac{1}{4} \tilde{\Phi}_{ai}^T \theta_i(Z_i) \hat{\Phi}_{ai} \vartheta_i^T(Z_i) \hat{\Phi}_{ci} + \tilde{\Phi}_{ai}^T \iota_{ai} \Phi_i \\ &- \tilde{\Phi}_{ai}^T \iota_{ai} \tilde{\Phi}_{ai} - \tilde{\Phi}_{ai}^T \iota_{ci} \bar{\vartheta}_i^T \Phi_i + \tilde{\Phi}_{ai}^T \iota_{ci} \bar{\vartheta}_i^T \tilde{\Phi}_{ci}. \end{aligned} \tag{37}$$

By using the definitions of λ_i and $\theta_i(Z_i)$, and combining (18), one has

$$\begin{aligned} \dot{V}_i &= \Phi_i^T \Psi_i(Z_i) \left(\mathcal{F}_i(e_i) - \frac{\dot{p}}{p} e_i \right) + \frac{1}{2} \Phi_i^T \theta_i(Z_i) \left(\Phi_i - \hat{\Phi}_{ai} \right) \\ &- \frac{1}{2} \Phi_i^T \theta_i(Z_i) \Phi_i + \Upsilon_{1i}(Z_i) + \tilde{\Phi}_{ci}^T \frac{\lambda_i}{(\lambda_i^T \lambda_i + 1)^2} \\ &\times \left(\frac{1}{4} \hat{\Phi}_{ai}^T \theta_i(Z_i) \hat{\Phi}_{ai} + \varepsilon_{HJB_i} - \lambda_i^T \tilde{\Phi}_{ci} \right) \\ &- \frac{1}{4} \tilde{\Phi}_{ai}^T \theta_i(Z_i) \hat{\Phi}_{ai} \vartheta_i^T(Z_i) \hat{\Phi}_{ci} + \tilde{\Phi}_{ai}^T \iota_{ai} \Phi_i \\ &- \tilde{\Phi}_{ai}^T \iota_{ai} \tilde{\Phi}_{ai} - \tilde{\Phi}_{ai}^T \iota_{ci} \bar{\vartheta}_i^T \Phi_i + \tilde{\Phi}_{ai}^T \iota_{ci} \bar{\vartheta}_i^T \tilde{\Phi}_{ci}, \end{aligned} \tag{38}$$

where

$$\Upsilon_{1i} = \varepsilon_i^T \left(\mathcal{F}_i - \frac{1}{2} g_i R_i^{-1} g_i^T \Psi_i^T \hat{\Phi}_{ai} - \frac{\dot{p}}{p} e_i \right). \tag{39}$$

Substitute λ_i into (17) and (26) yields

$$\begin{aligned}
 \dot{V}_i &= \Phi_i^T \lambda_{1i} + \frac{1}{2} \Phi_i^T \theta_i(Z_i) \tilde{\Phi}_{ai} + \Upsilon_{1i}(Z_i) \\
 &\quad - \frac{1}{4} \tilde{\Phi}_{ai}^T \theta_i(Z_i) \hat{\Phi}_{ai} \vartheta_i^T(Z_i) \hat{\Phi}_{ci} \\
 &\quad + \tilde{\Phi}_{ci}^T \frac{\lambda_i}{(\lambda_i^T \lambda_i + 1)^2} \left(\frac{1}{4} \hat{\Phi}_{ai}^T \theta_i(Z_i) \hat{\Phi}_{ai} + \varepsilon_{HJB_i} - \lambda_i^T \tilde{\Phi}_{ci} \right) \\
 &\quad + \tilde{\Phi}_{ai}^T \iota_{ai} \Phi_i - \tilde{\Phi}_{ai}^T \iota_{ai} \tilde{\Phi}_{ai} \\
 &\quad - \tilde{\Phi}_{ai}^T \iota_{ci} \bar{\vartheta}_i^T \Phi_i + \tilde{\Phi}_{ai}^T \iota_{ci} \bar{\vartheta}_i^T \hat{\Phi}_{ci} \\
 &= -y_i^T Q_i y_i - \frac{1}{4} \Phi_i^T \theta_i(Z_i) \Phi_i + \varepsilon_{HJB_i} \\
 &\quad + \frac{1}{2} \Phi_i^T \theta_i(Z_i) \tilde{\Phi}_{ai} \Upsilon_{1i}(Z_i) + \tilde{\Phi}_{ci}^T \frac{\lambda_i}{(\lambda_i^T \lambda_i + 1)^2} \\
 &\quad \times \left(\frac{1}{4} \hat{\Phi}_{ai}^T \theta_i(Z_i) \hat{\Phi}_{ai} + \varepsilon_{HJB_i} - \lambda_i^T \tilde{\Phi}_{ci} \right) \\
 &\quad - \frac{1}{4} \tilde{\Phi}_{ai}^T \theta_i(Z_i) \hat{\Phi}_{ai} \vartheta_i^T(Z_i) \hat{\Phi}_{ci} + \tilde{\Phi}_{ai}^T \iota_{ai} \Phi_i - \tilde{\Phi}_{ai}^T \iota_{ai} \tilde{\Phi}_{ai} \\
 &\quad - \tilde{\Phi}_{ai}^T \iota_{ci} \bar{\vartheta}_i^T \Phi_i + \tilde{\Phi}_{ai}^T \iota_{ci} \bar{\vartheta}_i^T \hat{\Phi}_{ci}.
 \end{aligned} \tag{40}$$

From $\tilde{\Phi}_{ci} = \Phi_i - \hat{\Phi}_{ci}$ and $\tilde{\Phi}_{ai} = \Phi_i - \hat{\Phi}_{ai}$, we have

$$\begin{aligned}
 &\frac{1}{4} \tilde{\Phi}_{ci}^T \frac{\lambda_i}{(\lambda_i^T \lambda_i + 1)^2} \tilde{\Phi}_{ai}^T \theta_i(Z_i) \tilde{\Phi}_{ai} \\
 &= \frac{1}{4} \tilde{\Phi}_{ai}^T \theta_i(Z_i) \tilde{\Phi}_{ai} \frac{\bar{\vartheta}_i^T}{ms} \Phi_i - \frac{1}{4} \tilde{\Phi}_{ai}^T \theta_i(Z_i) \Phi_i \frac{\bar{\vartheta}_i^T}{ms} \Phi_i \\
 &\quad + \frac{1}{4} \tilde{\Phi}_{ai}^T \theta_i(Z_i) \tilde{\Phi}_{ci} \frac{\bar{\vartheta}_i^T}{ms} \tilde{\Phi}_{ci} + \frac{1}{4} \tilde{\Phi}_{ai}^T \theta_i(Z_i) \hat{\Phi}_{ai} \frac{\bar{\vartheta}_i^T}{ms} \hat{\Phi}_{ci},
 \end{aligned} \tag{41}$$

where $ms = \lambda_i^T \lambda_i + 1$. Then, using (36), (37) can be rewrite as

$$\begin{aligned}
 \dot{V}_i &= -y_i^T Q_i y_i - \frac{1}{4} \Phi_i^T \theta_i(Z_i) \Phi_i + \varepsilon_{HJB_i} + \frac{1}{2} \Phi_i^T \theta_i(Z_i) \tilde{\Phi}_{ai} \\
 &\quad + \Upsilon_{1i}(Z_i) + \tilde{\Phi}_{ci}^T \bar{\vartheta}_i \left(-\bar{\vartheta}_i^T \tilde{\Phi}_{ci} + \frac{\varepsilon_{HJB_i}}{ms} \right) \\
 &\quad + \frac{1}{4} \tilde{\Phi}_{ai}^T \theta_i(Z_i) \tilde{\Phi}_{ai} \frac{\bar{\vartheta}_i^T}{ms} \Phi_i - \frac{1}{4} \tilde{\Phi}_{ai}^T \theta_i(Z_i) \Phi_i \frac{\bar{\vartheta}_i^T}{ms} \Phi_i \\
 &\quad + \frac{1}{4} \tilde{\Phi}_{ai}^T \theta_i(Z_i) \tilde{\Phi}_{ai} \frac{\bar{\vartheta}_i^T}{ms} \tilde{\Phi}_{ci} + \tilde{\Phi}_{ai}^T \iota_{ai} \Phi_i - \tilde{\Phi}_{ai}^T \iota_{ai} \tilde{\Phi}_{ai} \\
 &\quad - \tilde{\Phi}_{ai}^T \iota_{ci} \bar{\vartheta}_i^T \Phi_i + \tilde{\Phi}_{ai}^T \iota_{ci} \bar{\vartheta}_i^T \hat{\Phi}_{ci}.
 \end{aligned} \tag{42}$$

By Lemma 1, we know that $\frac{\dot{p}}{p}$ is bounded. Let c_{x_i} is the upper bound of $\left| \frac{\dot{p}}{p} \right|$, one can obtain

$$\begin{aligned}
 \|\Upsilon_{1i}\| &\leq (\delta c_{f_i} + c_{\zeta_i}) \|y_i\| \\
 &\quad + \frac{1}{2} \delta c_g^2 \sigma_{\max}(R^{-1}) c_{\Psi_i} \left(\|\Phi_i\| + \|\tilde{\Phi}_{ai}\| \right).
 \end{aligned} \tag{43}$$

According to [32], we know that ε_{HJB_i} converges to 0. select $\bar{\varepsilon}_{HJB_i} > 0$ such that $\sup_{X_i \in \Phi} \|\varepsilon_{HJB_i}\| < \bar{\varepsilon}_{HJB_i}$. Let $\tilde{X}_i = \left[y_i, \bar{\vartheta}_i^T \tilde{\Phi}_{ci}, \tilde{\Phi}_{ai} \right]^T$, (34) becomes

$$\begin{aligned}
 \dot{V}_i &\leq \frac{1}{4} \|\Phi_i\|^2 \|\theta_i(Z_i)\| + \bar{\varepsilon}_{HJB_i} + \frac{1}{2} \delta c_g^2 \sigma_{\max}(R^{-1}) c_{\Psi_i} \|\Phi_i\| \\
 &\quad - \tilde{X}_i^T M \tilde{X}_i + \tilde{X}_i^T d \\
 &= -\tilde{X}_i^T M \tilde{X}_i + \tilde{X}_i^T d + c,
 \end{aligned} \tag{44}$$

where $\sigma_{\max}(R^{-1})$ is the maximum eigenvalue of matrix R^{-1} ,

$$M = \begin{bmatrix} Q_i & 0 & 0 \\ 0 & 1 & (-\frac{1}{2}\iota_{ci}I2_{li} - \frac{1}{8ms}\theta_i\Phi_i)^T \\ 0 & -\frac{1}{2}\iota_{ci}I2_{li} - \frac{1}{8ms}\theta_i\Phi_i & \iota_{ai}I1_{li} - \frac{1}{8}(\theta_i\Phi_i\vartheta_i^T + \vartheta_i\Phi_i^T\theta_i) \end{bmatrix},$$

$$d = \begin{bmatrix} (\delta c_{f_i} + c_{x_i})I2_n \\ \frac{\bar{\epsilon}_{HJB_i}}{ms} \\ \left(\iota_{ai}I1_{li} + \frac{\theta_i}{2} - \iota_{ci}I2_{li}\bar{\vartheta}_i^T - \frac{\theta_i\Phi_i\vartheta_i^T}{4} \right) \varphi_i + \frac{\delta c_g^2 \sigma_{\max}(R^{-1}) c_{\Psi_i} I2_{li}}{2} \end{bmatrix},$$

$$c = \frac{1}{4} \|\Phi_i\|^2 \|\theta_i(Z_i)\| + \bar{\epsilon}_{HJB_i} + \frac{1}{2} \delta c_g^2 \sigma_{\max}(R^{-1}) c_{\Psi_i} \|\Phi_i\|$$

and $I1_{li} = \text{diag}\{1, \dots, 1\}$, $I2_{li} = [1, \dots, 1]^T$.

Using Sylvester's criterion [], one can obtain that $M > 0$ when $\iota_{ai}I1_{li} > \frac{1}{8}(\theta_i\Phi_i\vartheta_i^T + \vartheta_i\Phi_i^T\theta_i) + (\frac{1}{2}\iota_{ci}I2_{li} + \frac{1}{8ms}\theta_i\Phi_i) \times (-\frac{1}{2}\iota_{ci}I2_{li} - \frac{1}{8ms}\theta_i\Phi_i)^T$. Select ι_{ai} such that $M > 0$. Then, (40) becomes

$$\dot{V}_i \leq -\sigma_{\min}(M) \|\tilde{X}_i\|^2 + \|d_i\| \|\tilde{X}_i\| + c, \tag{45}$$

where $\sigma_{\min}(M)$ is the minimum eigenvalue of M .

If

$$\|\tilde{X}_i\| \geq \frac{d_i}{2\sigma_{\min}(M)} + \sqrt{\frac{d_i^2}{4\sigma_{\min}^2(M)} + \frac{c}{\sigma_{\min}(M)}} \triangleq B_{X_i}, \tag{46}$$

one has $\dot{V}_i \leq 0$, which means that $V_i \in L_\infty$, $y_i \in L_\infty$, $\tilde{\Phi}_{ci} \in L_\infty$, and $\tilde{\Phi}_{ai} \in L_\infty$ can be obtained. As $y_i \in L_\infty$, by (3), we have $-p < \|e_i\| < p$ which means that e_i can converge to Ω_e within a prescribed time T . By Lemma 1, one can obtain that the prescribed time synchronization of (1) and (2) are achieved. \square

5. Simulation

In this section, a numerical example [37] is given to verify the obtained results. The topology of driving network and response network is given in Figure 2.

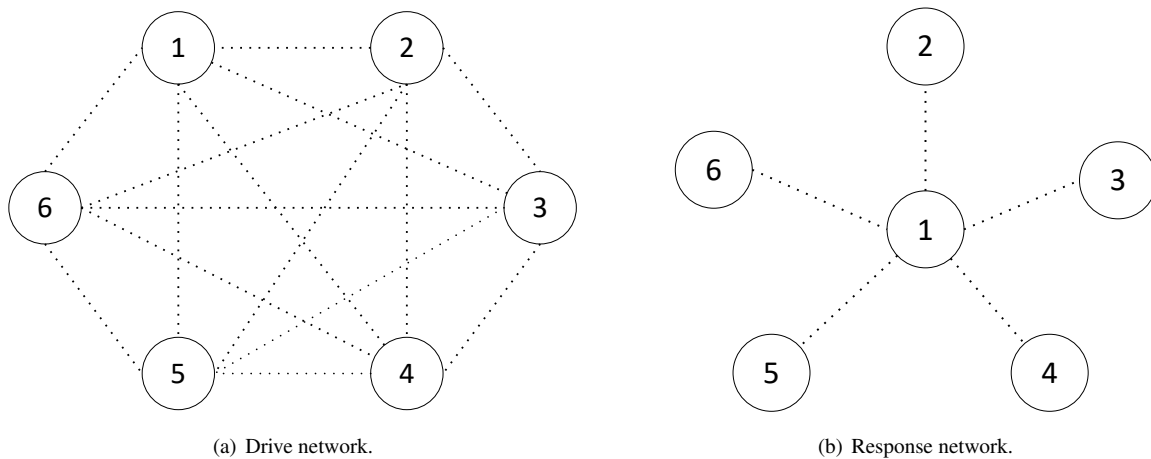


Figure 2. Comparison of drive and response networks.

The dynamics of driving network are as follows:

$$\dot{\zeta}_i = f_i(\zeta_i) + \sum_{j=1}^N a_{ij} H_1 \zeta_j, \tag{47}$$

where

$$f_i(\zeta_i) = \begin{bmatrix} -\zeta_{i1} + \zeta_{i2} \\ -0.5\zeta_{i1} - \zeta_{i1}(0.1\zeta_{i1} \sin(\zeta_{i2}) - \zeta_{i2})^2 \end{bmatrix}, \tag{48}$$

where $i = 1, \dots, 6$.

The dynamics of response network is as follows:

$$\dot{\xi}_i = z_i(\xi_i) + \sum_{j=1}^N c_{ij} H_2 \xi_j + g_i(\xi_i) u_i, \tag{49}$$

where

$$z_i(\xi_i) = \begin{bmatrix} -\xi_{i1} + \xi_{i2} - 3.5\xi_{i3} \\ -0.5\xi_{i1} - 0.5\xi_{i2} (1 - \cos(2\xi_{i2} + 2))^2 + \sin(\xi_{i3})^2 \\ \xi_{i1}^3 + \sin(\xi_{i2}^2) - \xi_{i3} - \xi_{i2}^4 \end{bmatrix}, \tag{50}$$

$$g_i(\xi_i) = \begin{bmatrix} 0.5 & 0 & 0 \\ 0 & \cos(2\xi_{i1} + 2) & 0 \\ 0 & 0 & \sin(\xi_{i2}) \end{bmatrix}. \tag{51}$$

By (4), one has $e_i = (e_1, e_2, e_3)^T, i = 1, \dots, 6$. The topology of two networks is given in Fig.2a and Fig.2b. Then, we have: $a_{ij} = 1 (i = 1, \dots, 6, j = 1, \dots, 6, i \neq j), a_{11} = a_{22} = a_{33} = a_{44} = a_{55} = a_{66} = -5, c_{11} = -5, c_{22} = c_{33} = c_{44} = c_{55} = c_{66} = -1, c_{12} = c_{21} = 1, c_{13} = c_{31} = 1, c_{14} = c_{41} = 1, c_{15} = c_{51} = 1, c_{16} = c_{61} = 1$. Let the inner coupling matrix $H_1 = \text{diag}\{0.1, -0.1\}$ and $H_2 = \text{diag}\{0.1, -0.2, 0.1\}, B =$

$$\begin{bmatrix} -1 & 0 \\ -1 & 0.64 \\ -0.51 & -0.85 \end{bmatrix}.$$

The fuzzy sets of FNN $\Psi^T(Z) \hat{\Phi}_c$ are defined as $[-3, 3]$. Let $Z = [e, p, y]^T$, and for $k = 1, 2, \dots, 7$ define $Z^0 = \left[\underbrace{[-4+k, -4+k, -4+k]^T, \dots, [-4+k, -4+k, -4+k]^T}_3 \right]^T$ the fuzzy membership functions are designed as $\mu_{F^k}(Z) = \exp\left(-\frac{(Z-Z^0)^T(Z-Z^0)}{2}\right)$. The fuzzy basis function are defined $\Psi(Z) = [\Psi^1, \Psi^2(Z), \dots, \Psi^7]$, and $\Psi^k = \frac{\mu_{F^k}(Z)}{\sum_{k=1}^7 \mu_{F^k}(Z)}$. Let $Q = R = I_3$. We initialize the system with $\zeta_k(0) = [\frac{k}{N}, \frac{k}{N}]^T, \xi_k(0) = [\frac{k}{N}, \frac{k}{N}, \frac{k}{N}]^T, k = 1, \dots, N$. The initial values for (16) and (21) are set as $\hat{\Phi}_c(0) = [0.2]_{7 \times 1}, \hat{\Phi}_a(0) = [0.3]_{7 \times 1}, \varpi_1 = 1, \varpi_2 = 1, \iota_a = 5, \text{ and } \iota_c = 0.7, -0.1 < \tau < 0.1, T = 9$.

The simulation results are given in Figures 3–5. Figure 3 gives the trajectory of the projective synchronization error $e_i = (e_1, e_2, e_3)^T, i = 1, \dots, 6$. It can be seen that e_i converges to the expected accuracy $-0.1 < \tau < 0.1$ within $T = 9$. Figure 4 shows the trajectory of the performance function of all nodes. Figure 5 shows the evaluation network trajectory Φ_{ci} of nodes 1 and 5. Figure 6 shows the control strategy trajectory u of node 5. From Figures 3–6, it can be concluded that the projective synchronization between (47) and (48) is achieved within $T = 9$.

To demonstrate the superiority of the proposed method, we compare our algorithm with three reinforcement learning-based control approaches: fuzzy RL [36], adaptive RL (ARL) [15], and standard RL [38]. The performance value are illustrated in Figure 7. The control input of different methods are shown in Figure 8. The corresponding tracking error are depicted in Figure 9. The quantitative comparison of key performance metrics, including convergence time, synchronization error, and control effort, is summarized in Table 1. It can be observed that our method has better performance and faster convergence speed than the three existing methods.

Table 1. Performance metrics for different control methods.

Control Method	Convergence Time (s)	Synchronization Error (RMSE)	Control Effort (IAE)
Standard RL [38]	12.1	0.098	0.7
Fuzzy RL [36]	14.2	0.087	2.4
Adaptive RL (ARL) [15]	16.8	0.072	1.7
Proposed Method	9.0	0.042	0.2

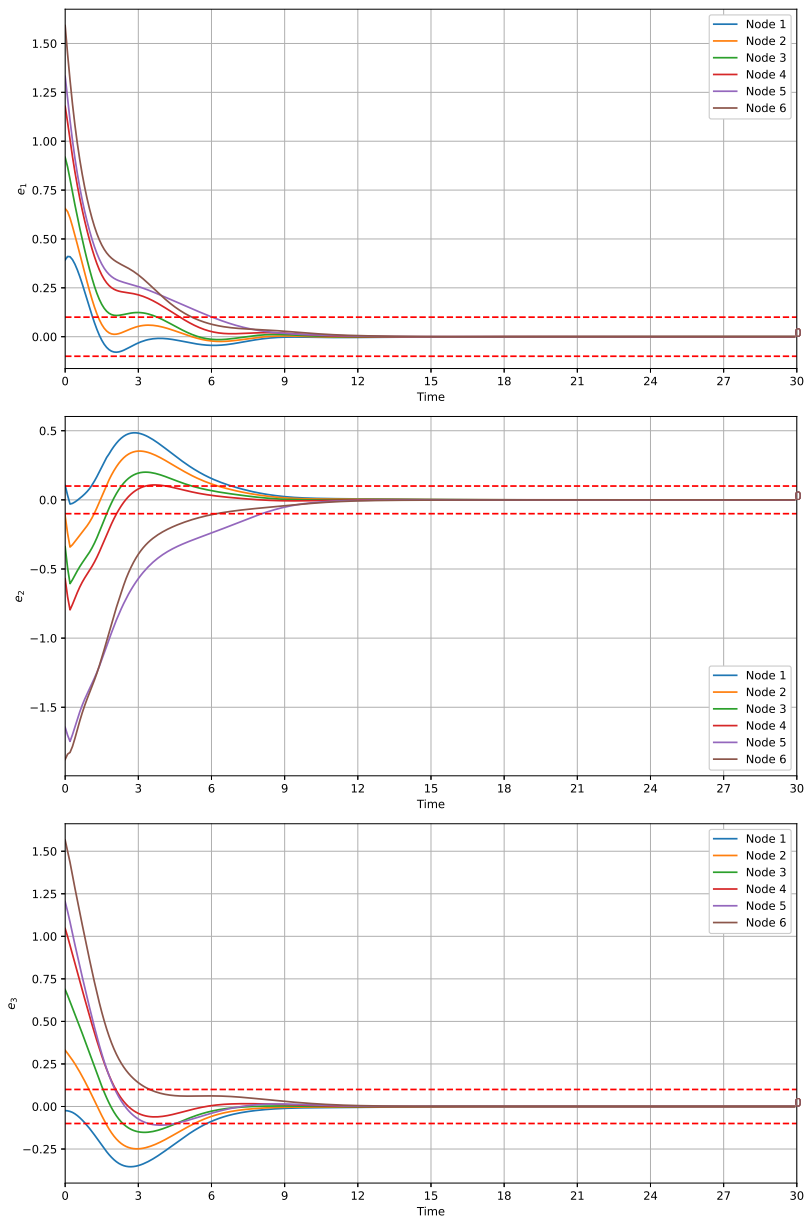


Figure 3. The trajectories of synchronization error.

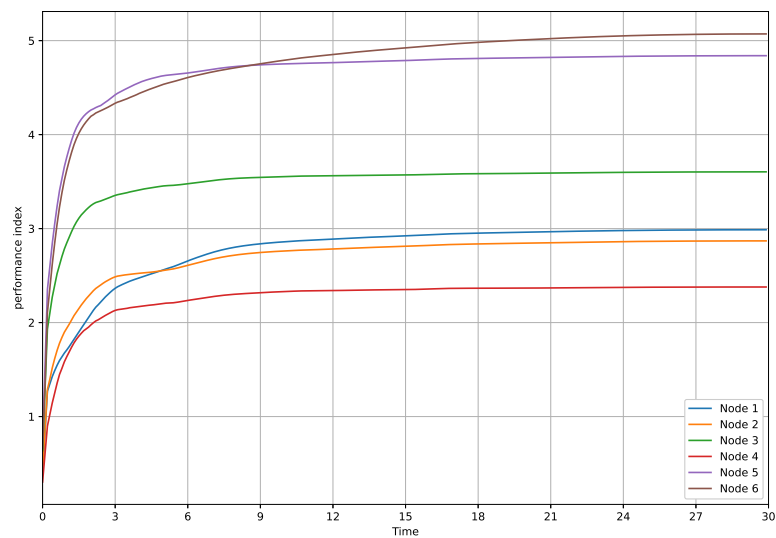


Figure 4. The trajectory of the performance function of all nodes.

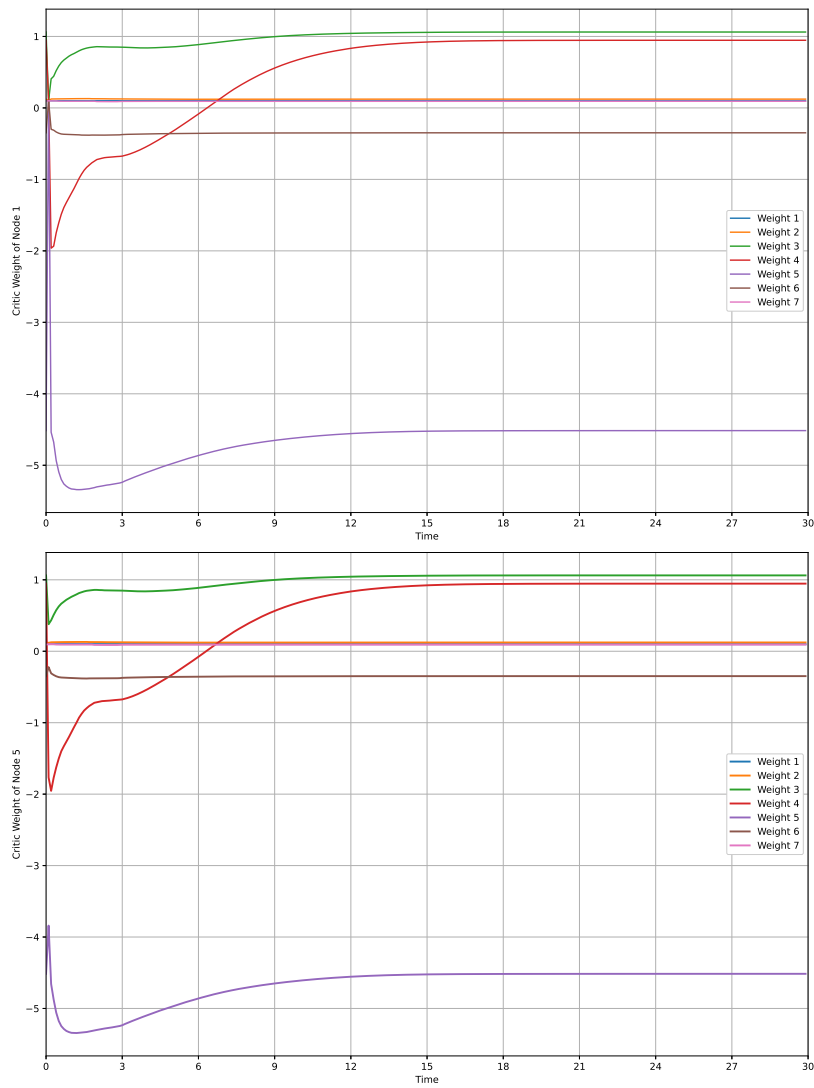


Figure 5. Weights of critic.

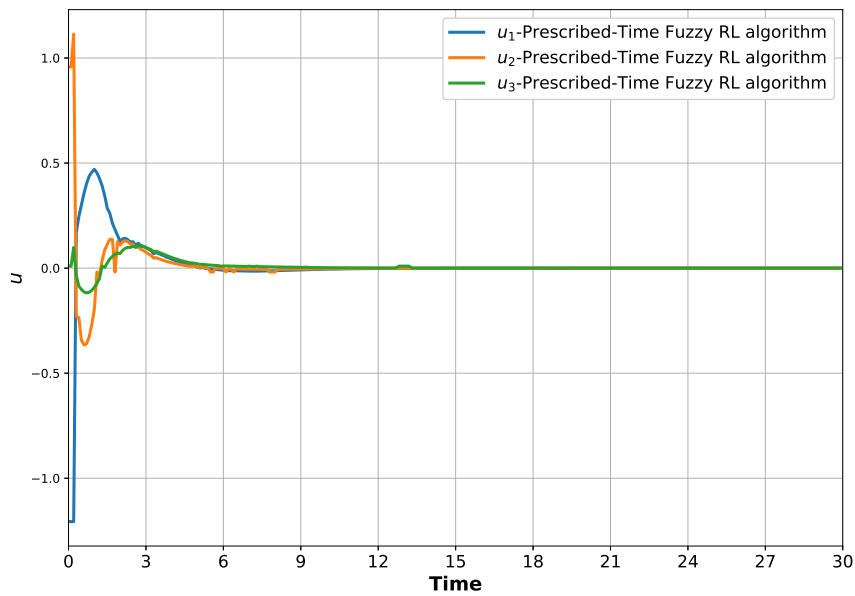


Figure 6. Trajectories of control policy u .

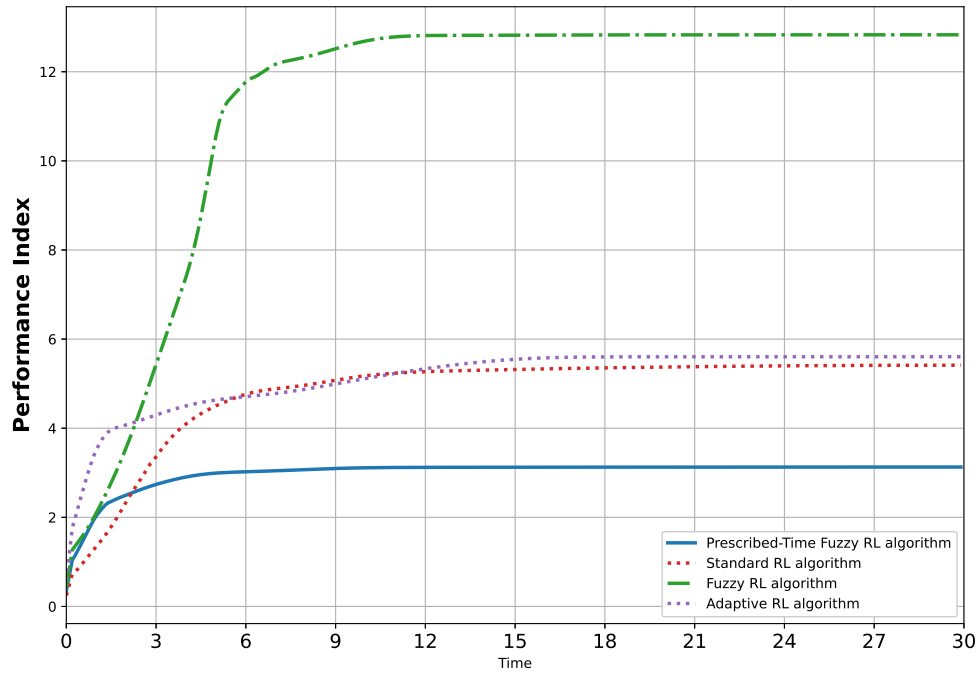


Figure 7. The node trajectory of the performance function for PTFRL, FRL, RL, ARL.

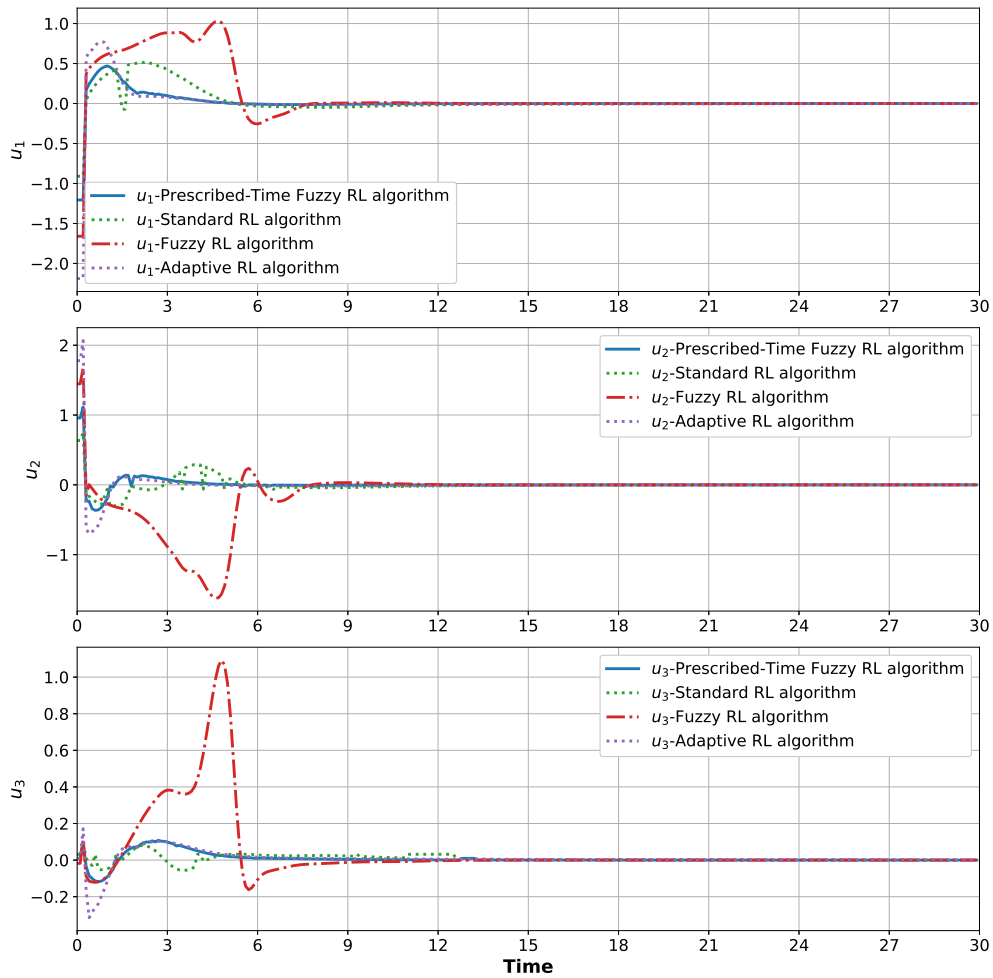


Figure 8. The node trajectory of u for PTFRL, FRL, RL, ARL.

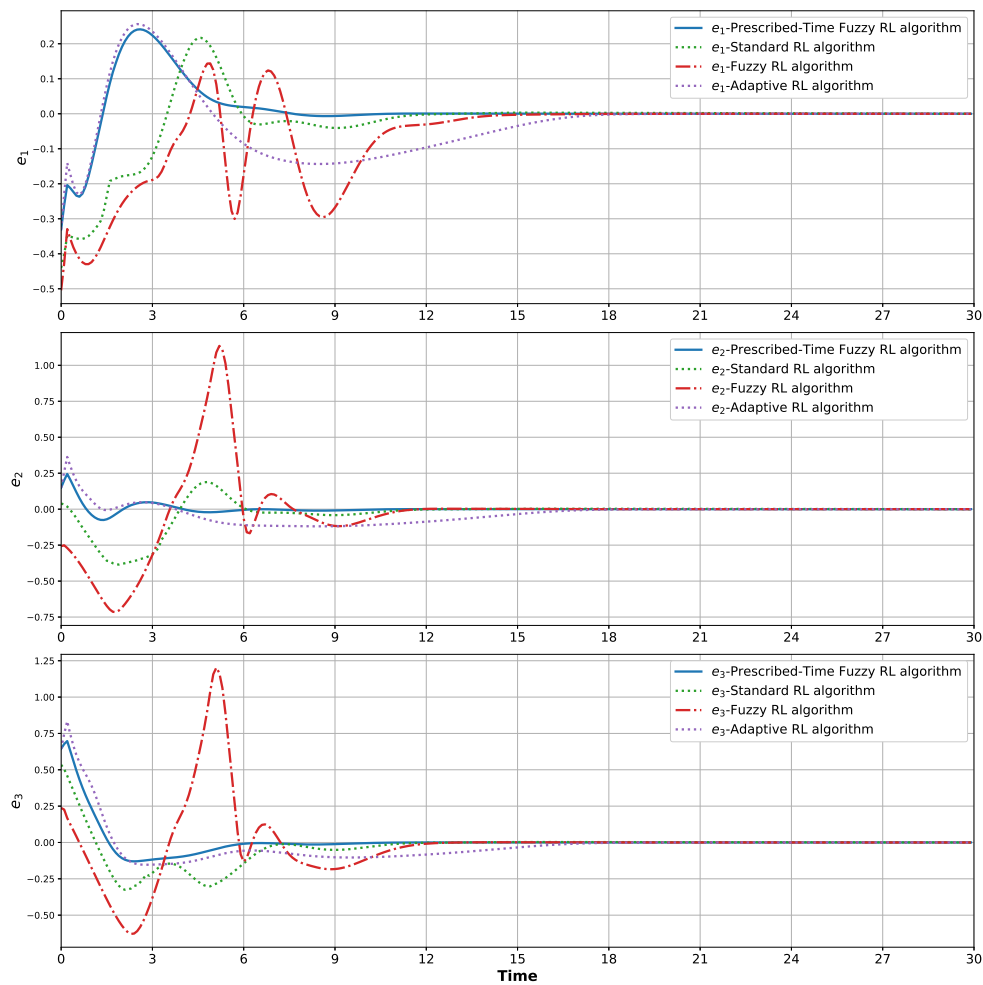


Figure 9. The node trajectory of e for PTFRL, FRL, RL, ARL.

6. Conclusions

This paper investigates the prescribed-time projective synchronization problem for complex networks (CNs) with nodes of different dimensions. A projective synchronization error is first formulated, and a novel performance value function incorporating prescribed-time constraints and accuracy requirements is introduced. A fuzzy controller based on an A fuzzy actor-critic neural network (FACNN) framework is then developed to address the prescribed-time synchronization challenge. Furthermore, rigorous convergence analysis is provided, proving that the synchronization error converges to a predefined residual set within the prescribed time, independent of initial conditions. Finally, a numerical example is presented to validate the effectiveness of the proposed approach, demonstrating that the synchronization objective is achieved as expected.

Author Contributions

X.Q.: conceptualization, methodology, software, data curation, writing—original draft preparation; T.D.: supervision, writing—reviewing and editing. All authors have read and agreed to the published version of the manuscript.

Funding

This research received no external funding.

Institutional Review Board Statement

Not applicable.

Informed Consent Statement

Not applicable.

Data Availability Statement

Not applicable.

Conflicts of Interest

The authors declare no conflict of interest.

Use of AI and AI-Assisted Technologies

No AI tools were utilized for this paper.

Appendix A

In this section, we proof Lemma 1.

Proof. For $0 \leq t < T$, get

$$\dot{p} = -2 \frac{(1-\tau)(T-\tau)}{T^2} < 0. \tag{A1}$$

So p is strictly decreasing over $[0, T)$, with $p(0) = 1$, and $p = \tau$ for $\forall t \geq T$; Since p is defined at T , from (6),

$$\lim_{t \rightarrow T^-} p = \lim_{t \rightarrow T^+} p = p(T) = \tau. \tag{A2}$$

By (6), we can obtain that

$$\dot{p}_-(T) = \dot{p}_+(T) = 0. \tag{A3}$$

So, \dot{p} exists at T . Using (6), the has

$$\dot{p} = \begin{cases} -2(1-\tau) \frac{T-\tau}{T} + \tau, & 0 \leq t < T \\ 0, & t \geq T. \end{cases} \tag{A4}$$

This means that $\lim_{t \rightarrow T^-} \dot{p}(t) = \lim_{t \rightarrow T^+} \dot{p}(t) = 0$, i.e., \dot{p} is continuous for all $t \geq 0$. Since, $\dot{p}(0) = \frac{-2(1-\tau)}{T}$, we have that \dot{p} is bounded. Therefore, both p and \dot{p} are bounded and p is continuously differentiable. Moreover, by (6) and (43), we have that

$$\frac{\dot{p}}{p} = \begin{cases} \frac{-2(1-\tau)T-\tau}{(1-\tau)(T-t)^2+\tau T^2}, & 0 \leq t < T \\ 0, & t \geq T \end{cases}. \tag{A5}$$

From (A2), one can obtain

$$\lim_{t \rightarrow T^-} \frac{\dot{p}}{p} = \lim_{t \rightarrow T^+} \frac{\dot{p}}{p} = \frac{\dot{p}}{p}(T) = 0. \tag{A6}$$

Since, $\frac{\dot{p}}{p}(0) = -2(1-\tau)/T$ and $\frac{\dot{p}}{p}$ is continuous, it can be concluded that $\frac{\dot{p}}{p}$ is bounded. □

References

1. Wu, J.; Xia, Y. Complex-Network-Inspired Design of Traffic Generation Patterns in Communication Networks. *IEEE Trans. Circuits Syst. II Express Briefs* **2016**, *64*, 590–594.
2. Xuan, Q.; Zhang, Y.Z.; Fu, C. Social Synchrony on Complex Networks. *IEEE Trans. Cybern.* **2017**, *48*, 1420–1431.
3. Chen, Z.; Wu, J.; Xia, Y. Robustness of Interdependent Power Grids and Communication Networks: A Complex Network Perspective. *IEEE Trans. Circuits Syst. II Express Briefs* **2017**, *65*, 115–119.
4. Rubinov, M.; Sporns, O. Complex Network Measures of Brain Connectivity: Uses and Interpretations. *Neuroimage* **2010**, *52*, 1059–1069.
5. Guo, W.; Toader, B.; Feier, R. Global Air Transport Complex Network: Multi-Scale Analysis. *SN Appl. Sci.* **2019**, *1*, 680.
6. Li, B.; Wang, Z.; Ma, L. An Event-Triggered Pinning Control Approach to Synchronization of Discrete-Time Stochastic Complex Dynamical Networks. *IEEE Trans. Neural Netw. Learn. Syst.* **2018**, *29*, 5812–5822.
7. Wang, L.; Wang, Z.; Huang, T. An Event-Triggered Approach to State Estimation for a Class of Complex Networks with Mixed Time Delays and Nonlinearities. *IEEE Trans. Cybern.* **2015**, *46*, 2497–2508.
8. Dong, T.; Wang, A.J.; Zhu, H.Y.; et al. Event-Triggered Synchronization for Reaction–Diffusion Complex Networks via Random Sampling. *Phys. Stat. Mech. Its Appl.* **2018**, *495*, 454–462.
9. Dong, H.L.; Zhou, J.M.; Wang, B.C. Synchronization of Nonlinearly and Stochastically Coupled Markovian Switching Networks via Event-Triggered Sampling. *IEEE Trans. Neural Netw. Learn. Syst.* **2018**, *29*, 5691–5700.

10. Tang, Z.; Park, J.H.; Shen, H. Finite-Time Cluster Synchronization of Lur'e Networks: A Nonsmooth Approach. *IEEE Trans. Syst. Man, Cybern. Syst.* **2017**, *48*, 1213–1224.
11. Liu, X.; Chen, T. Finite-Time and Fixed-Time Cluster Synchronization with or Without Pinning Control. *IEEE Trans. Cybern.* **2016**, *48*, 240–252.
12. Tan, M.; Tian, W. Finite-Time Stabilization and Synchronization of Complex Dynamical Networks with Nonidentical Nodes of Different Dimensions. *Nonlinear Dyn.* **2015**, *79*, 731–741.
13. Zhang, C.; Wang, X.Y. Robust Outer Synchronization Between Two Nonlinear Complex Networks with Parametric Disturbances and Mixed Time-Varying Delays. *Phys. Stat. Mech. Its Appl.* **2018**, *494*, 251–264.
14. Lin, D.; Liu, J.M.; Zhang, F. Adaptive Outer Synchronization of Delay-Coupled Nonidentical Complex Networks in the Presence of Intrinsic Time Delay and Circumstance Noise. *Nonlinear Dyn.* **2015**, *80*, 117–128.
15. Fan, A.; Li, J. Adaptive Neural Network Prescribed Performance Matrix Projection Synchronization for Unknown Complex Dynamical Networks with Different Dimensions. *Neurocomputing* **2018**, *281*, 55–66.
16. Jian, L.X.; Guang, Y.H. Adaptive Fault-Tolerant Synchronization Control of a Class of Complex Dynamical Networks with General Input Distribution Matrices and Actuator Faults. *IEEE Trans. Neural Netw. Learn. Syst.* **2015**, *28*, 559–569.
17. Wu, Y.B.; Fu, S.X.; Li, W.X. Exponential Synchronization for Coupled Complex Networks with Time-Varying Delays and Stochastic Perturbations via Impulsive Control. *J. Frankl. Inst.* **2019**, *356*, 492–513.
18. Wen, Z. Synchronization of Stochastic Dynamical Networks Under Impulsive Control with Time Delays. *IEEE Trans. Neural Netw. Learn. Syst.* **2013**, *25*, 1758–1768.
19. Wang, X.; Liu, X.; She, K. Delay-Dependent Impulsive Distributed Synchronization of Stochastic Complex Dynamical Networks with Time-Varying Delays. *IEEE Trans. Syst. Man, Cybern. Syst.* **2018**, *49*, 1496–1504.
20. Li, X.; Wang, N.; Lu, J. Pinning Outer Synchronization of Partially Coupled Dynamical Networks with Complex Inner Coupling Matrices. *Phys. Stat. Mech. Its Appl.* **2019**, *515*, 497–509.
21. Huang, H.; Xu, J.; Wang, J.; et al. Reinforcement Learning-Based Secure Synchronization for Two-Time-Scale Complex Dynamical Networks with Malicious Attacks. *Appl. Math. Comput.* **2024**, *479*, 128840.
22. Zhang, H.; Yan, D.; Zhang, Y.; et al. Distributed Synchronization Based on Model-Free Reinforcement Learning in Wireless ad Hoc Networks. *Comput. Netw.* **2023**, *227*, 109670.
23. Yu, X.; Khani, A.; Chen, J.; et al. Real-Time Holding Control for Transfer Synchronization via Robust Multiagent Reinforcement Learning. *IEEE Trans. Intell. Transp. Syst.* **2022**, *23*, 23993–24007.
24. Li, M.; Qin, J.; Ma, Q.; et al. Hierarchical Optimal Synchronization for Linear Systems via Reinforcement Learning: A Stackelberg-Nash Game Perspective. *IEEE Trans. Neural Netw. Learn. Syst.* **2021**, *32*, 1600–1611.
25. Zhou, Z.; Liu, Y.; Lu, J.; et al. Cluster Synchronization of Boolean Networks Under State-Flipped Control with Reinforcement Learning. *IEEE Trans. Circuits Syst. II Express Briefs* **2022**, *69*, 5044–5048.
26. Qin, J.; Li, M.; Shi, Y.; et al. Optimal Synchronization Control of Multiagent Systems with Input Saturation via Off-Policy Reinforcement Learning. *IEEE Trans. Neural Netw. Learn. Syst.* **2019**, *30*, 85–96.
27. Li, K.; Yang, L.; Guan, C.; et al. Reinforcement Learning-Based Pinning Control for Synchronization Suppression in Complex Networks. *Heliyon* **2024**, *10*, e34065.
28. Zhong, M.; Huang, C.; Cao, J.; et al. Adaptive Fuzzy Echo State Network Optimal Synchronization Control of Hybrid-Order Chaotic Systems via Reinforcement Learning. *Chaos Solitons Fractals* **2024**, *181*, 114665.
29. Zhou, Z.; Liu, Y.; Cao, J.; et al. Cluster Synchronization of Boolean Control Networks with Reinforcement Learning. *IEEE Trans. Circuits Syst. II Express Briefs* **2023**, *70*, 4434–4438.
30. Guleva, V. Node Correlation Effects on Learning Dynamics in Networked Multiagent Reinforcement Learning. In Proceedings of the 6th Scientific School Dynamics of Complex Networks and their Applications, Kaliningrad, Russia, 14–16 September 2022; pp. 110–113.
31. Wang, W.; Feng, C.; Quan, W. Data-Driven Control of a Class of Discrete-Time Linear Complex Dynamical Networks. In Proceedings of the IEEE International Conference on Big Data, Los Angeles, CA, USA, 9–12 December 2019; pp. 6243–6245.
32. Destro, A.; Giorgi, G. Reinforcement Learning Applied to Network Synchronization Systems. In Proceedings of the IEEE International Symposium on Measurements & Networking, Padua, Italy, 18–20 July 2022; pp. 1–6.
33. Dong, T.; Gong, X.; Li, H.; et al. Data-Driven Tracking Control for Multi-Agent Systems with Unknown Dynamics via Multithreading Iterative Q-Learning. *IEEE Trans. Syst. Man, Cybern. Syst.* **2023**, *53*, 2533–2542.
34. Dong, T.; Li, K.; Huang, T. Event-Based ADP Tracking Control of Complex-Valued Nonlinear Systems. *IEEE Trans. Emerg. Top. Comput. Intell.* **2024**, *8*, 1086–1096.
35. Shen, Z.; Dong, T.; Huang, T. Asynchronous Iterative Q-Learning Based Tracking Control for Nonlinear Discrete-Time Multi-Agent Systems. *Neural Netw.* **2024**, *180*, 106667.
36. Wang, L.X.; Mendel, J.M. Fuzzy Basis Functions, Universal Approximation, and Orthogonal Least Squares Learning. *IEEE Trans. Neural Netw.* **1992**, *3*, 807–814.
37. Hu, W.; Gao, L.; Dong, T. Event-Based Projective Synchronization for Different Dimensional Complex Dynamical Networks with Unknown Dynamics by Using Data-Driven Scheme. *Neural Process. Lett.* **2021**, *53*, 3031–3048.

38. Sheng, L.; Yang, H. Exponential Synchronization of a Class of Neural Networks with Mixed Time-Varying Delays and Impulsive Effects. *Neurocomputing* **2008**, *71*, 3666–3674.
39. Li, J.; Pei, X.; Ji, L. Data-Based Optimal Couple-Group Consensus Control for Heterogeneous Multi-Agent Systems via Policy Gradient Reinforcement Learning. *Journal of Machine Learning and Information Security* **2026**, *2* (1), 1.
40. Tang, H.; Wang, Y.; Li, B.; Deng, J.; Zhang, Z. Bayesian Local Differential Privacy for Implicit Feedback Recommendation. *Journal of Machine Learning and Information Security* **2025**, *1* (1), 6.
41. Shao, Y.; Li, Y.; Wu, B. A Directional Attention Fusion and Multi-Head Spatial-Channel Attention Network for Facial Expression Recognition. *Journal of Machine Learning and Information Security* **2025**, *1* (1), 7.